Microscopic Analysis of Prefinitely Strained Cement Paste


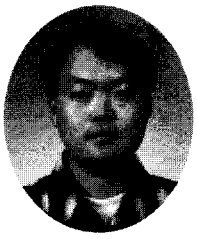
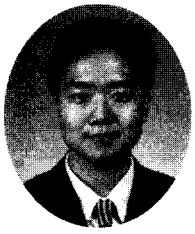


Song, Ha-Won* Kim, Jang-Ho** Choi, Jae-Hyeok*** Byun, Keun-Joo****

ABSTRACT

In this paper, a microscopic analysis of prefinitely strained cement paste specimen was carried out. The microscopic behavior of concrete under triaxial stress must be fully understood in order to explain the additional ductility that comes from lateral confinement and to get microstructural information in large deformed and large strained concrete. The so-called "tube-squash" test was applied to achieve enormously high shear and deviatoric strain of concrete under extremly high pressure without fracture. Then, microscopic analyses by focusing on hydration and microstructure of prefinitely strained cement paste were carried out on cored-out deformed and virgin (undeformed) cement paste specimens: the first specimen being 40 days old, the second one being one year old. The microscopic analysis by Field Emission Scanning Electronic Microscope (FESEM) was carried out for comparison between the specimens after 40 days and those after one year. For one year old specimens, X-Ray Diffractometer (XRD) analysis, Energy Dispersive x-ray Spectrometer (EDS) analysis, and Differential Thermal Analysis/Thermo-Gravity (DTA/TG) analysis were also carried out to study the hydration and the microstructures of prefinitely strained cement paste specimen by focusing on the methodologies of their microscopic analyses.

Keywords : microscopic analysis, large strained cement paste, tube squash test, FESEM, microstructure, hydration, XRD, EDS, DTA/TG

* Associate Prof., Dept. of Civil Eng., Yonsei University, Korea
** Assistant Prof., Dept. of Civil and Environ. Eng., Sejong University, Korea
*** Graduate Student, Dept. of Civil Eng., Yonsei Univercity, Korea
**** Prof., Dept. of Civil Eng., Yonsei University, Korea

1. INTRODUCTION AND THEORY

It is well known fact that lateral confinement on quasi-brittle materials increases ductility. The additional ductility comes from the enforcement of the triaxial stress state on the quasi-brittle material. In other words, the triaxial stress condition limits the initiation of tensile cracks and the damage localization at stresses far exceeding the tensile strength of the material. In concrete, most widely used quasi-brittle material, the application of confinement by lateral reinforcements and retrofitting composite columns are a few examples among many cases where the ductility is maximized. Even in the extreme loading conditions such as earthquakes and missile penetration, various types of lateral reinforcements are used to prevent ultimate catastrophic failure as well as maintain structural serviceability in concrete structures.

As early as 1905, Woolson[1] discovered the increased ductility of concrete using lateral reinforcements. The results of standard triaxial tests done by Balmer[2] and Bazant et. al.[3] also shows the ductility increase due to the lateral confinement. The compression tests of concrete reinforced by stirrups were also carried out by Burdette and Hillsdorf to show the ductility increase[4]. Park and Paulay[5] proposed constitutive equations considering the confinement effect of concrete. Bazant et. al.[6] obtained experimentally hydrostatic stress-strain relations of concrete and hardened cement paste up to record pressures of 2069 MPa in confined uniaxial-strain compression tests.

Although the application of confinement to achieve high ductility in cementitious materials has been extensively studied, the understanding of material behavior which results in increased ductility has been lacking. In order to explain the additional ductility that comes from lateral confinement, microscopic behavior of the cementitious material under triaxial stress condition must be fully understood. For example, the way in which the hydration process unfolds during the formation of cement paste is critical in gaining the knowledge of concrete ductility. After the initial curing process of cement and water has been achieved, the rehydration of unhydrated cement particles and residual water molecules or free water within the paste during the extreme straining case has to be further studied. In this study, a microscopic analysis is carried out for so-called the experimental specimens obtained from the filled-tube squash test of concrete by Kim[7]. In their analysis cement paste has been cast in a highly ductile steel tube and deformed to half of the its original length. Then, the inner core of this filled tube specimen has been cored out immediately after the prestraining. By applying extreme straining of 50% axial strain and 70° diagonal shear angle rotation during the prestraining stage of the experiment, the extreme microscopic condition can be obtained.

In a FESEM (Field Emission Scanning Electron Microscope) analysis, microscopic photos of both inplane and cross-section specimens of deformed and virgin types both taken after 40 days from initial casting and taken after one years are analyzed. For the one year old specimens, microscopic photos of various magnifications—to observe the constituents (C-S-H hydrate, micropore, microcrack, etc.) at the suitable magnifications—were taken in the microstructures[8] of the cement paste specimens. To get the objectivity, over 200 photos were taken for the 4 specimens—inplane deformed, inplane virgin,

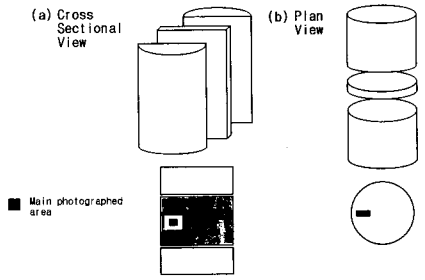

Fig.1 Specimen Preparation for Microscopic Analysis

cross-section deformed, cross-section virgin specimens, respectively--which cover overall area except extremely bell shaped part (Fig.1). An XRD (X-Ray Diffractometer) analysis for the one year specimens was also done for comparing the relative intensity of $Ca(OH)_2$ between the inplane and virgin deformed specimen. An EDS (Energy Dispersive x-ray Spectrometer) analysis for one year specimens was performed to get information of the amounts of atomic components. A DTA/TG (Differential Thermal Analysis/Thermo-Gravity) analysis was also carried out to get the quantity of $Ca(OH)_2$ and C-S-H (Calcium Silicate Hydrate) in the microstructures of the one year old specimen. By observing both hydration percentage and formation of microstructure, we attempt to understand the microstructural behavior of prefinitely strained cement paste.

Table 1 Mixture content of each material

Content	HSC	NSC	Cement Paste	Cement Mortar
Cement-type I (kgf)	459.03	356.48	1570.52	1178.7
Pea-Max.0.625cm(kgf)	1020.66	997.03		
Sand-No.2 (kgf)	793.66	931.55		1496.52
S.F. Slurry (kgf)	128.11			
Water (kgf)	117.70	211.85	628.52	504.44
Superplasticize (mL)	160.0			
	per m^3			

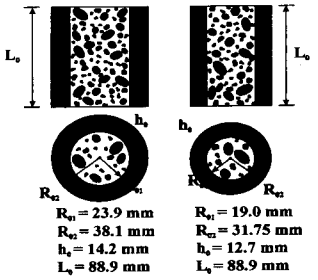

Fig.2-(a) Filled tube specimen dimensions

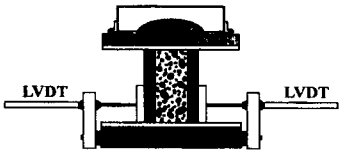

Fig.2 (b) Setup of LVDT to measure lateral displacement during the compression

2. EXPERIMENTAL METHOD

2.1 Basic Characteristics of the Tube-Squash Test

Two series of tests were carried out using steel alloy tubes of two different diameters which dimensions are shown in Fig. 2a. The tubes were made of steel alloy ASTM No. 1020. The normal strength concrete (NSC) has maximum aggregate size of 9.52 mm and average uniaxial compression strength f_c'=41.37 MPa. The mix design of concrete and other cementitious materials is shown in Table 1. The high strength concrete (HSC) had maximum aggregate size of 9.52 mm, and uniaxial compression strength f_c'=86.19 MPa. The specimens were cast and cured at room temperature in a water bath for 28 days, after which, they were tested. For the tube-squash test, the maximum lateral displacement is continuously measured by LVDT as shown in Fig.2b. The tests were carried out at

constant rate of axial displacement, The diameters of the cores drilled from the specimens were 31.623 mm and 25.273 mm, respectively.

Fig.3 shows the axial cut through a specimen of high strength concrete squashed to 50% of its original length. The rearrangement and flattening of the aggregate pieces caused by shortening of the tube to half the length can be seen. No visual cracks or voids are detected even though initially orthogonal diagonals have changed their angle by 70 degree.

Fig.4a shows, on the right, the diagrams of axial load versus axial displacement between the specimen ends and, on the left, the lateral displacement for the squash test of larger and smaller diameter tubes, respectively. A graph for the unfilled steel tubes is also shown in Fig.4a. The corresponding diagrams of the axial stress versus the axial strain and the lateral strain for the larger and smaller diameter tubes are shown in Fig.4b, respectively.

A squashed filled tube of the smaller diameter from which a core has been drilled out. For comparison tests, identical cores were drilled out of virgin concrete specimens cast from the same batch of concrete. Fig.5 shows pairs of the cores extracted from normal concrete, high-strength concrete, cement mortar and hardened cement paste. The deformed concrete is on the left of each pair, and

Fig.3 The cross sectional photo of high strength concrete filled tube specimen after 50% compression

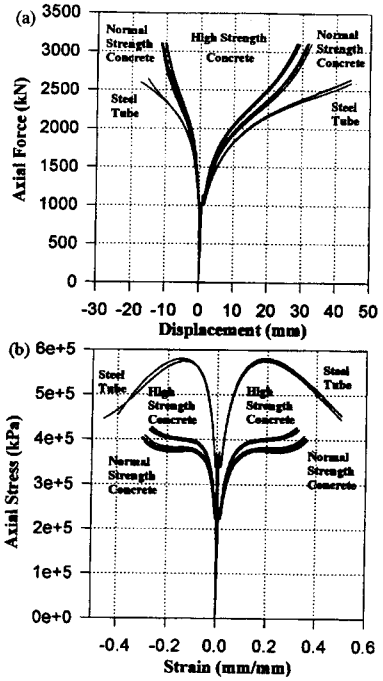

Fig.4 (a) Axial force versus axial and radial displacement diagrams and (b) Axial stress versus axial and radial strain diagrams for larger diameter filled tube specimens

the virgin concrete on the right in each figures.

After removing the squashed tube specimens from the testing machine, three types of examination are conducted. Some specimens are cut and the surface of concrete is examined visually (Fig.3).

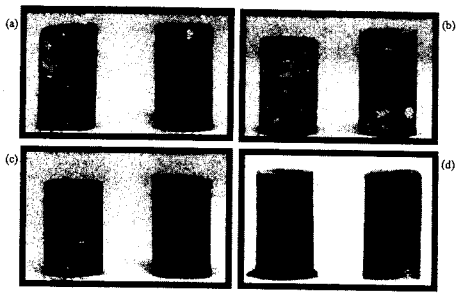

Fig.5 Cores of deformed and virgin material of (a) normal strength concrete, (b) high strength concrete, (c) cement mortar, (d) cement paste

Although the possibility to attain good ductility in concrete by high confining pressure has been well known, the strain magnitude that can be attained without any visually observable damage is at first startling. Even after undergoing a shear angle over 70 degree, the surface of a cut specimen's concrete core show no voids or fractures. A coring machine is used to drill out cores from the remaining specimens in the axial direction. These cylindrical cores are then subjected either to the uniaxial compression test or to the Brazilian split cylinder test. The tests yield the stress-strain curves, compression strength and splitting tensile strength of the highly deformed concrete; See Kim[7] for further details. The specimen taken from the cement paste cores are used for this study.

2.2 Basic Characteristics of the Microscopic Analysis

The main focus of this study is the microscopic analysis of cored-out cement paste specimen from the tube-squash test. The hardened cement paste cast in the steel tube and deformed to 50% of its original length is analyzed microscopically to study microstuctures of prefinitely strained cement in paste. By studying prestrained cement paste at microscopic level and comparing the mechanical behavior with concrete filled tube specimen, we can relate the aggregate and cement matrix contributions to the deformation process and explain the increased ductility of the material.

As explained earlier, the specimens are prepared by slicing in two principal directions of cross sectional cut and planal cut as shown in Fig.1. Since the compression and the deformations of the filled tube specimen follow the initial principal axis, the displacement profile can be considered as axis symmetric.

In this research, a microscopic analysis for one yaer old cement paste specimens is studied. The FESEM using Hitachi Model S-4200 was used for the analysis. Electron gun is Cold Emission Type. Accelerating voltage is 0.5-30kV. Magnification is over 500,000x. Lens system is Electromagnetic & cornical type. Vaccum system is ion & DP & Rotary. It has antivibrational system. The EDS is with FESEM. It has No LN_2 cooling type and detector resoultion is under 140eV. Jawed et. al.[9] explained the hydration of portland cement, and described the C-S-H type in the SEM analysis. C-S-H type I is like "needles radiating from grain", type II is "reticulated", type III is "indefinite" and type IV is "spherical agglomerates." Reinhardt[10] explained the mechanism of hydration of cement focusing the C-S-H in details. The observation of the C-S-H is the main concern. In this SEM analysis, in order to clearly observe hydration products, 5,000x, 10,000x, 15,000x and 50,000x magnified photos have been taken. 5,000x and 10,000x are very profitable to observe several hydration products. From 15,000x, one kind of hydration products (for example, the C-S-H hydration products) can be focused very well. So not to lose the trend, under 10,000x is suitable.

Procedure of SEM Specimen preparation is as follows; Using diamond blade saw, the slicing in inplane and cross section is made for both virgin and deformed cement paste immediately after the "tube-squash" test and coring has been completed after 28 days from casting. In the inplane, the mid-section where the maximum strain has been applied is sliced out. In the cross section, also the mid-section has been sliced out. Once the slicing has been done, the sections are embedded in the

resin-epoxy for the easier handling during the grinding and minimum polishing process required for the preparation of the microscopic analysis. The thin layer of Pt-Pd coating has to be applied to the surface of the specimen. And the specimens are stored under vacuum in order to be most effectively observed in FESEM. Using various magnifications of 300x, 600x, 5,000x, 10,000x, 15,000x and 50,000x the microscopic photos are taken at various locations of the specimen. In order to show the inherent axis-symmetric geometrical deformation profile, the photos are taken at various angles with a constant radius from the center of the specimen. In the inplane case of the 40 days observation, the location of the taken photo is determined by the area where the tensile cracking gradually disappears. In the observation, 300x and 600x magnifications are used to observe the crack, and 5,000x, 10,000x, 15,000x, 50,000x magnifications are used for the hydration observation. An EDS analysis is done and mapping is performed for noticeable area.

For XRD and DTA/TG analysis for one year specimens, cement paste specimens were crushed to pieces—become powder, until it feels very soft, then the specimen is attached to the receptacle.

3. RESULTS AND DISCUSSION

3.1 FESEM Analysis

· 40days old specimen

From the 300x magnification photos taken after 40 days from the initial casting, two trends can be observed as shown in Fig.6. The inplane photos of virgin and deformed specimens show distinct difference in the microcrack propagation. Even though microcracks can be detected in the virgin specimen, the microcracks are inherent shrinkage cracks and are not compression prestraining produced cracks. However, the microcracks observed in inplane deformed specimen are due to the prestraining compression where the large tensile strain in the mid-section of the specimen initiated the microcrack and propagated toward the center of the specimen (Fig.6a). More specifically, the microscopic photo of the deformed specimen can be divided into 3 layers. The most outer layer contains several distinct microcracks. As the crack converges toward the center of the specimen, a transition layer, where the microcracks gradually disappear, emerges. Following the transition layer, the center part of the specimen contains only the inherent microcracks and the tension derived cracks do not exist. When the photos of the virgin and deformed specimens of both inplane and cross-section together are compared the rehydration of unhydrated cement paste or partially hydrated cement paste (dehydration) taken place during the prestraining compression can be expected. The light gray areas of the photos are assumed to represent the partially hydrated or unhydrated cement paste. In the virgin specimen photo, the light gray particles are scattered throughout the photo. However, in the a deformed specimen, the percentage of the light gray area is reduced and the remaining unhydrated cement particles are converged into larger lumps. Also the light gray areas in the transition zone of the inplane deformed photograph have relatively flat shape differing from the other 2 zones.

· One year old specimen

From all photos taken from one year old specimens over 5000x magnification for hydration observation as shown in Figs.7, 8 and 9, it is expected that hydration is more proceeded than 40 days old specimen even irrespective of the deformed or virgin

(a) inplane deformed specimen (300x)

(b) inplane virgin specimen (300x)

(c) x-section deformed specimen (300x)

(d) x-section virgin specimen (300x)

Fig.6 40 days old specimens

Fig.7 Inplane deformed one year old specimen

point a (10,000x)

point b (10,000x)

point b (50,000x)

point d (10,000x)

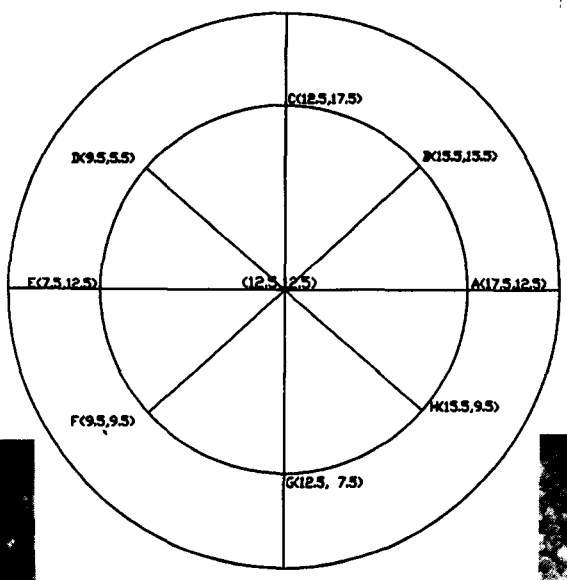

axis

point d (50,000x)

point e (10,000x)

point e (50,000x)

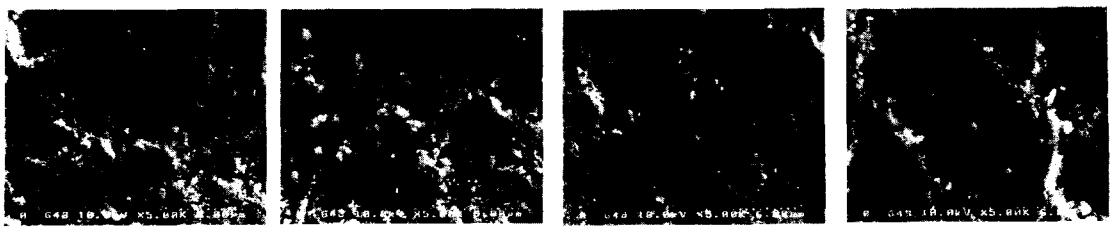

point e (5,000x) point b (5,000x) point d (5,000x) point a (5,000x)

Fig.8 Cross-section deformed one year old specimen(use same axis as Fig.7)

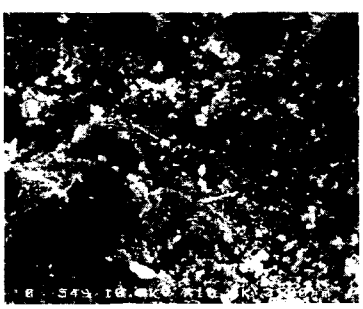

point e (10,000x)

point e (50,000x)

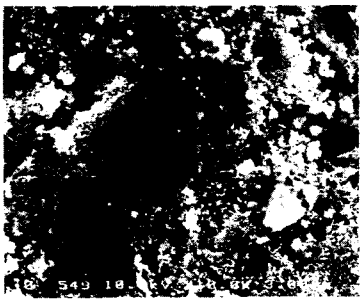

point g (10,000x)

point g (50,000x)

point h (10,000x)

point h (50,000x)

Fig.9 Inplane virgin one year old specimen (use same axis as Fig.7)

specimens. There are large difference between the deformed and virgin specimen in hydration product, type and density of C-S-H and hydration rate, in both in-plane and cross-section. In the case of deformed specimen photos (Figs.7 and 8), it is observed that few C-S-H type I can be seen and almost every C-S-H type was non-crystalline type III. However, in virgin specimen photos over 10,000x (Fig.9), there are a lot of hydration products of C-S-H type I. In the case of inplane deformed specimen (Fig.7), the enlargement of C-S-H type III area is noticeable as like rock scattered shape. The C-S-H type I and II can be observed just a little amount (at a few parts). Microcracks and micropores can be observed in the photos. In the observation, the deformed specimens both inplane and cross-section have more micropores than the virgin specimen. This rock scattered shape of the C-S-H type III enlargement, microcracks, micropores seem to show loose microstructures of deformed specimens.

In the case of inplane virgin specimen (Fig.9), the C-S-H type I can be seen easily in almost all photos. The C-S-H type III also can be seen. However, the shapes between inplane virgin and deformed specimen are noticeably different. The inplane virgin specimen has more complex products than the deformed. Microcracks and micropores can be seen in almost all photos.

In the case of cross-section deformed specimen (Fig.8), it has similar trend with inplane deformed specimen. However the amount of C-S-H type III in cross-section deformed specimen is lower than that of inplane deformed specimen.

From the observation with lower magnification (300x and 600x), several microcracks can be observed in all photos as shown in Figs.10 and 11. This microcracks cannot be noticed by naked eyes. However, in the inplane deformed one year old specimen, the distinct microcracks of the outer layer as at inplane deformed 40 days old specimen could not be observed. The well-focused, representative photos of inplane deformed and virgin specimens with several magnifications are shown for comparison in Figs.12 and 13.

3.2 EDS Analysis

During the FESEM analysis, an EDS analysis was done at a cracked area of the inplane deformed specimen (Fig.14). The Ca/Si ratio is about 1.7~1.8. We can see the scattered area of Ca and Si in spot mapping image (Fig.15). At Ca and Si distribution charts as shown in Fig.15, in many parts, the white spots in the Si chart coupled each other with the white spots in the Ca chart, even though there are more white spots in the Ca chart. Also Al and Mg can be seen. However, between Si and Al or Si and Mg, a few parts coupled. It proves that Ca and Si coexists even they are not the C-S-H hydrate. However, many Al and Mg do not coexist with Si. It is expected that Al and Mg are not familiar with Si in cement pate chemically or physically.

3.3 XRD Analysis

For both cross-section inplane deformed specimen and virgin specimen powder, an XRD analysis is performed, The fig.16 shows that the intensity of $Ca(OH)_2$ hydration products is different. At different angles of 18° and 34° .

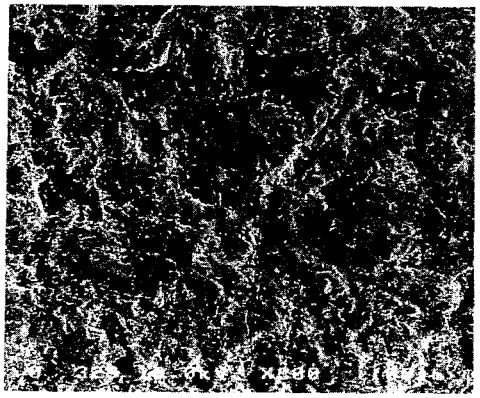

point (0,0) (300x) (inplane deformed)

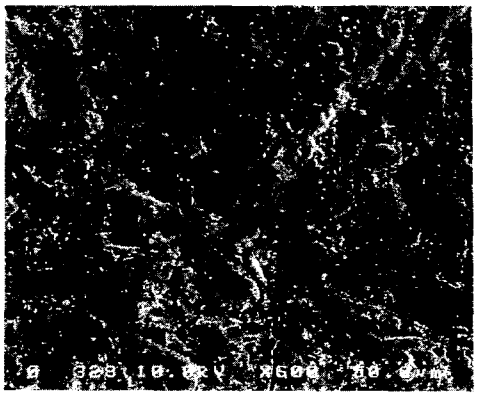

point (0,0) (600x) (inplane deformed)

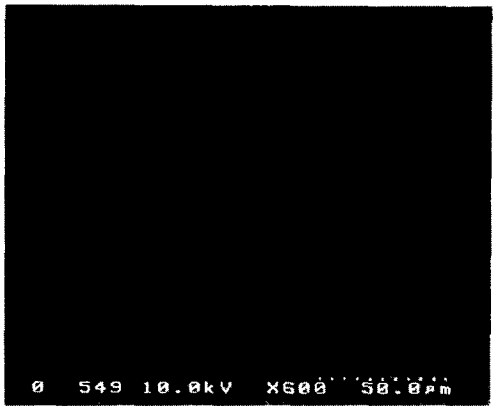

point (15.5, 9.5) (600x) (inplane deformed)

point (21, 8) (600x) (cross-section deformed)

Fig.10 Deformed one year old specimen (use same axis as Fig.7)

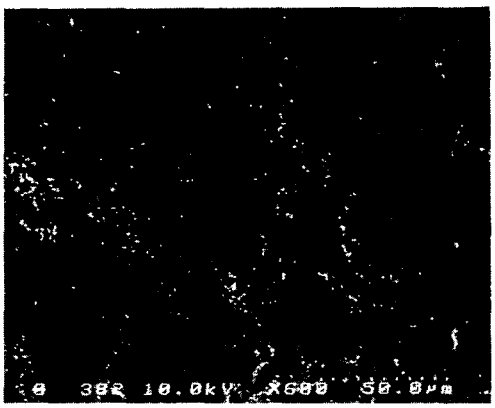

point (6,15) (600x) (inplane virgin)

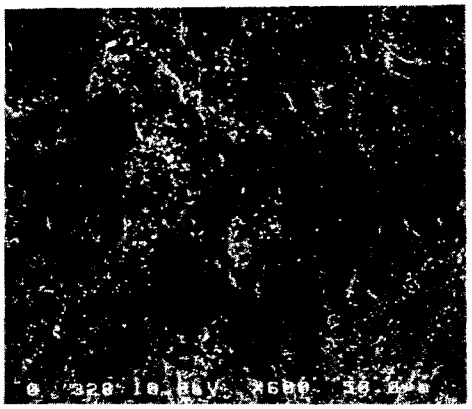

point e (600x) (inplane virgin)

Fig.11 Virgin one year old specimen (use same axis as Fig.7)

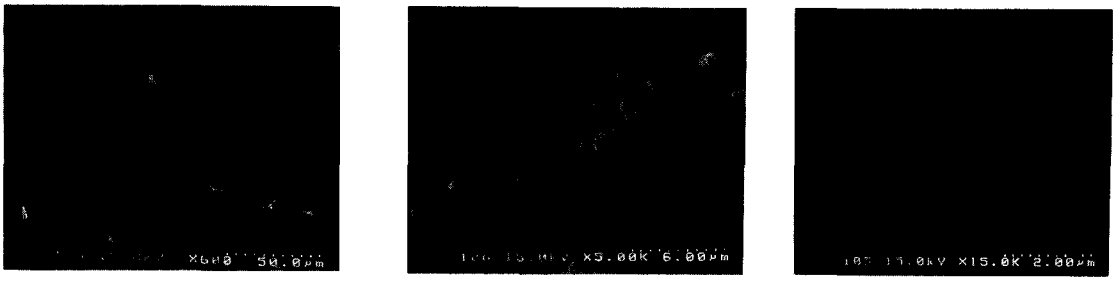

(a) 600x (b) 5,000x (c) 15,000x

Fig.12 Well-focused inplane deformed one year old specimen

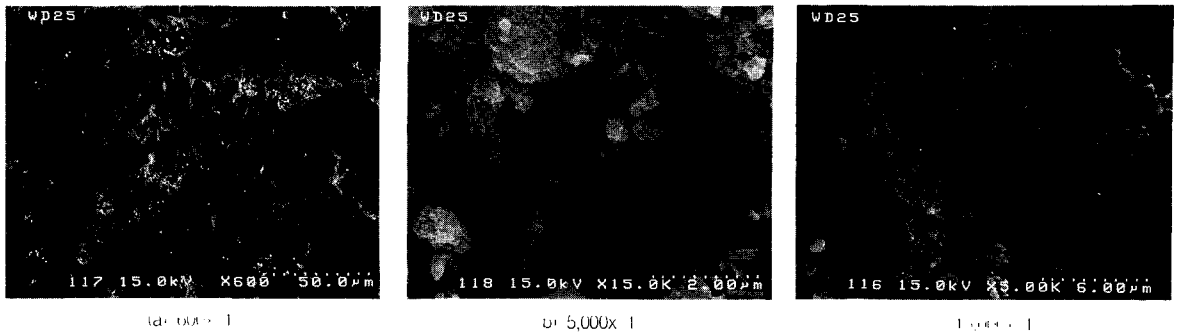

(d) 5,000x 2 (e) 15,000x-2

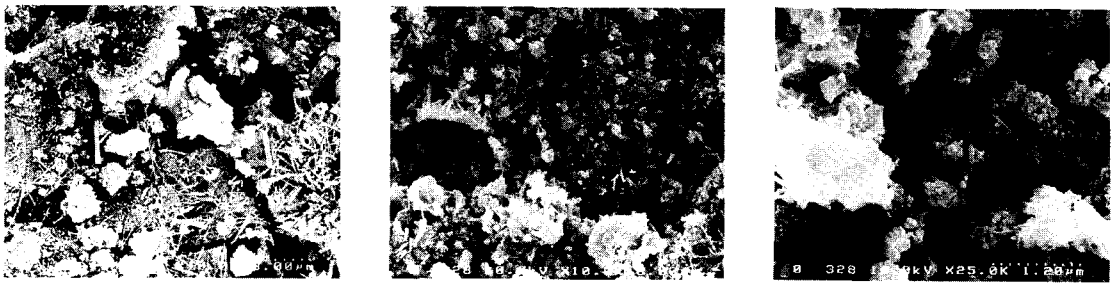

(f) 10,000x-3 (g) 10,000x-4 (h) 25,000x-5

Fig.13 Well-focused inplane virgin one year old specimen

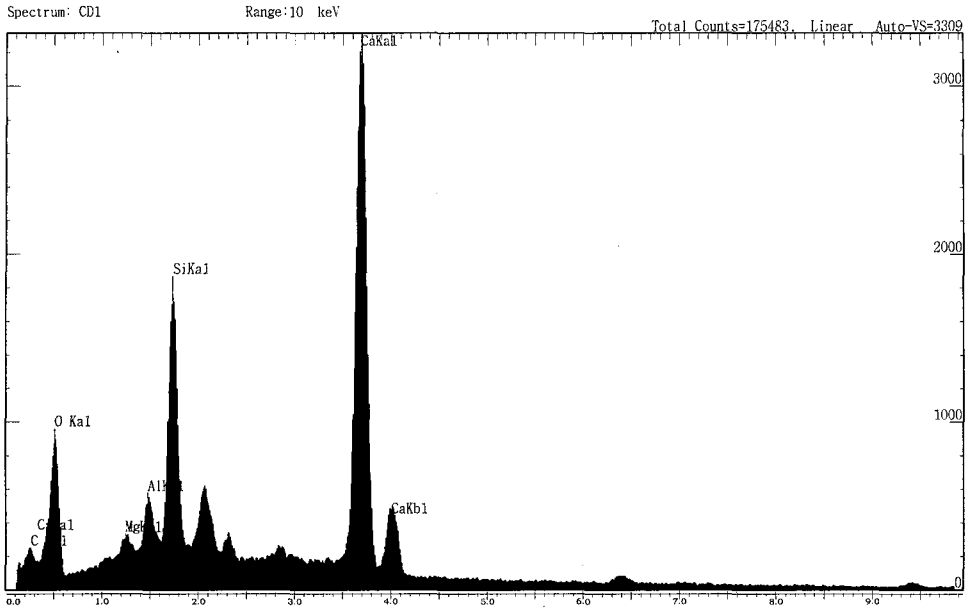

Fig.14 EDS data

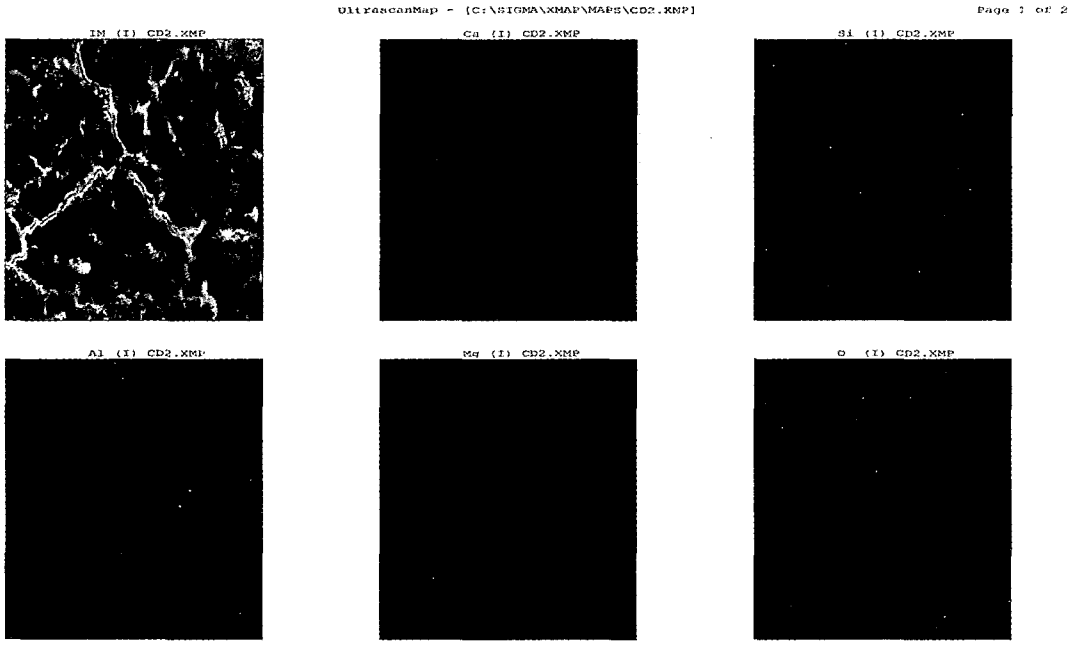

Fig.15 EDS area mapping

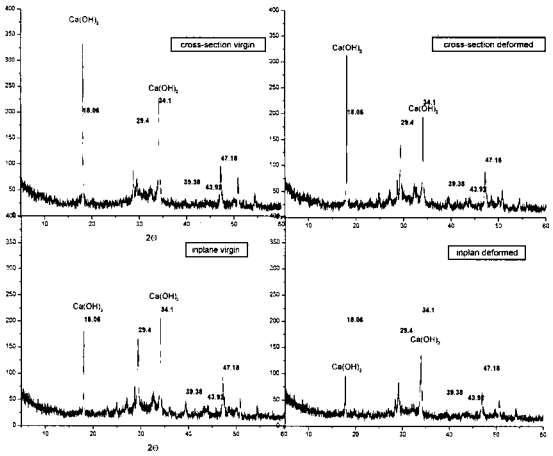

Fig.16 XRD graph for every type

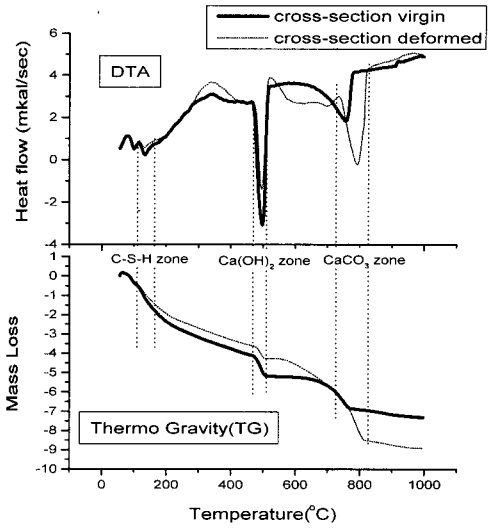

Fig.17 DTA/TG analysis

The intensity of $Ca(OH)_2$ at the cross section virgin specimen powder is higher than the cross section deformed. Same trend can be observed from the comparison between the inplane deformed and virgin specimen powder. It can be expected that the amount of hydrate and the degree of hydration of the virgin specimens are higher than those of the deformed. To get more and exact information, DTA/TG is then performed.

3.4 DTA/TG Analysis

For the cross-section deformed and virgin cement paste specimen powder, a DTA/TG analysis is performed. As shown in Fig.17, the hydration rate of the virgin powder is higher than that of the deformed powder in the C-S-H zone and the $Ca(OH)_2$ zone. However, in the $CaCO_3$ zone, the trend has been changed i.e., the amount of $CaCO_3$ in the deformed is higher than in the virgin. So, it can be expected that more micropores have been formed during the deformation process so that the microstructures become looser than that of the virgin, which makes CO_2 gas penetrate more easily at the deformed.

4. CONCLUSION

The following conclusions are obtained from this study.

1) Tube squash test of cement paste proves that the large deformation and 50% large strain confined by steel are possible without failure.

2) In the 300x FESEM analysis of the 40 days old inplane deformed specimen, we can observe 3 layers. These are the outer part where are the distinct microcracks, the transition part, and the inner part, in which microcracks are very different from the distinct microcraks in the outer part. Also, there are noticeable difference in the width of the grey color area, which is assumed to represent unhydrated portions, between the inplane deformed and inplane virgin specimen. The grey area of the inplane virgin

specimen is larger than that of the inplane deformed.

3) From the FESEM analysis of the one year old specimen over 5000x, the C-S-H type I and III are observed in virgin specimen, however, in the deformed specimen C-S-H type III is mainly observed. More micropores are observed in the deformed specimen, From the FESEM analysis using 300x, 600x for the one year old specimen, we observed microcracks which is invisible by the naked eyes. The EDS analysis informed the ratio of Ca and Si, and the mapping shows visually where the each atom exists.

(4) The XRD analysis shows the relative difference of $Ca(OH)_2$ between the inplane deformed and inplane virgin specimen. The DTA/TG analysis shows the different hydration rates of C-S-H and $Ca(OH)_2$ between the deformed and the virgin which observed in the XRD on $Ca(OH)_2$ i.e., lower hydration rates as in the deformed specimens for the one year old specimen, The opposite trend on amount of $Ca(CO)_3$ from the DTA/TG analysis is obtained, i.e., the micropores of the deformed specimen due to deformation make the CO_2 gas penetrate more easily than those of virgin specimen, so that more carbonation may occur.

REFERENCES

1. Woolson, I.H., "Some Remarkable Tests indicating Flow of Concrete under Pressure." *Engrg.News*, 54 (18), 1905, pp. 459-460.
2. Balmer, G.G., *Shearing Strength of Concrete under High Triaxial Stress Computation of Mohr's Envelope as Curve*, Report SP-23, Structural Research Laboratory, *Bureau of Reclamation*, U.S. Dept. of the Interior, Denver, Colorado. 1949.
3. Bazant, Z.P.,Xiang, Y., Adley, M.D., Prat, P.C., and Agers, S.A.(1996). "Microplane Model for Concrete, Part II:Data Delocalization and Verification." *J. of Engrg. Mech ASCE*, 122(3), 1990, pp. 255-262
4. Burdette, E.G., and Hilsdorf, H.K., "Behavior of Laterally Reinforced Concrete Colums," *J. of struct. Engrg. ASCE*. Feb., 1971, pp. 587-602
5. Park, R., and Paulay, T., *Reinforced Concrete Structrures*, John Wiley and Sons, Inc., New York. 1975.
6. Bazant, Z.P., Bishop, F.C., and Chang, T.-P. "Confined Compression Tests of Cement Paste and Concrete up to 3000ksi." *ACI Materials J.*, 33 (July-August), 1986, pp. 553-560
7. Kim, Jang-Ho J., *Failure Mechanism and Size Effect of Quasi-Brittle Materials: Ice, Steel Reinforced Concrete, and Fiber Composite*, Ph. D. Dissertation, Northwestern University, 1998, pp. 7-20.
8. Metha. P.Kumar, *Concrete*, Prentice-Hall, Inc. A Simon & Schuster Company Englewood Cliffs, New Jersey. 1993, pp. 17-42.
9. Jawed, I., Skalny, J., and Young J.F., "Hydration of Portland Cement", *Structure and Performance of Cements*, Applied Science Publishers, London and New York., 1983, pp. 237-317
10. Reinhardt. H.W., "Relation Between the Microstructure and Structural Performance of Concrete", A. Aguado, R. Gettu and S.P. Shah(eds.) *Concrete Technology: New Trends, Industrial Applications.*, E&FN Spon, London. 1994, pp. 19-30